HHS Public Access

Author manuscript

J Immunol. Author manuscript; available in PMC 2015 September 15.

Published in final edited form as:

J Immunol. 2015 March 15; 194(6): 2587–2595. doi:10.4049/jimmunol.1400326.

Quantitative reduction of the T cell receptor adapter protein SLP-76 unbalances immunity and immune regulation

Owen M. Siggs[*,†,1,2], **Lisa A. Miosge**[*,1], **Stephen R. Daley**[*,1], **Kelly Asquith**[‡], **Paul S. Foster**[‡], **Adrian Liston**[§], and **Christopher C. Goodnow**[*,2]

[*]Department of Immunology, John Curtin School of Medical Research, The Australian National University, Canberra 2601, Australia

[†]Wellcome Trust Sanger Institute, Hinxton, Cambridge CB10 1SA, UK

[‡]Priority Research Centre for Asthma and Respiratory Diseases, School of Biomedical Sciences and Pharmacy, University of Newcastle, Callaghan, NSW 2300, Australia

[§]Department of Microbiology and Immunology, VIB and University of Leuven, Leuven 3000, Belgium

Abstract

Gene variants that disrupt T cell receptor signaling can cause severe immune deficiency, yet less disruptive variants are sometimes associated with immune pathology. Null mutations of the gene encoding the scaffold protein SLP-76, for example, cause an arrest of T cell positive selection, while a synthetic membrane-targeted allele allows limited positive selection but is associated with proinflammatory cytokine production and autoantibodies. Whether these and other enigmatic outcomes are due to a biochemical uncoupling of tolerogenic signaling, or simply a quantitative reduction of protein activity, remains to be determined. We describe here a splice variant of *Lcp2* that reduced the amount of wild-type SLP-76 protein by ~90%, disrupting immunogenic and tolerogenic pathways to different degrees. Mutant mice produced excessive amounts of proinflammatory cytokines, autoantibodies and IgE, revealing that simple quantitative reductions of SLP-76 were sufficient to trigger immune dysregulation. This allele reveals a dose-sensitive threshold for SLP-76 in the balance of immunity and immune dysregulation: a common disturbance of atypical clinical immune deficiencies.

Keywords

T Cell Receptor; Tolerance; Immunodeficiency Diseases; Autoimmunity

[2]Address correspondence to: Owen M. Siggs, Wellcome Trust Sanger Institute, Hinxton, Cambridge CB10 1SA, UK, T: +44(0)1865287793, F: +44(0)1865287787, owen.siggs@sanger.ac.uk or Christopher C. Goodnow, Department of Immunology, John Curtin School of Medical Research, GPO BOX 334, Canberra City ACT 2601, Australia, T: +61(0)261252596, F: +61(0)261252595, chris.goodnow@anu.edu.au.

[1]O.M.S., L.A.M. and S.R.D. contributed equally to this work.

Introduction

Exome sequencing has revealed that our protein coding genomes are spectacularly diverse, with new variants emerging in every generation (1). Many of these variants have no effect on the proteins they encode, while others inactivate them completely. The remainder fall between these two extremes, and lead instead to qualitative or quantitative effects on protein function. In the context of the immune system, we have learned a great deal from the study of null alleles in mice, and continue to do so with the rapid expansion and systematic phenotyping of public knockout mouse resources (2). Yet we understand far less about variants with intermediate effects, despite their frequency and capacity to cause or modify human disease.

Antigen recognition by the T cell receptor is a case in point, where null alleles in mice and humans have allowed a fine dissection of the pathway (3). Absence of the proximal kinase ZAP-70, for example, disrupts thymic positive selection and peripheral T cell activation, leading to severe immune deficiency in mice and in humans (4–7). More enigmatic is the outcome of missense variation in ZAP-70, which in several cases displays paradoxical associations between immune deficiency and autoimmune pathology (8, 9). The *Zap70*^{W163C} variant in mouse, for example, impairs TCR signaling and positive selection, yet in the correct genetic and environmental context will cause autoimmune arthritis (8, 10). The use of an allelic series of hypomorphic *Zap70* variants has established that immune dysregulation can result from stepwise reductions in ZAP-70 activity (9, 11–14), likely due to its differential contribution to immunity versus tolerance. As another example, deficiency of the transmembrane adapter protein LAT blocks T cell development in mice (15), yet missense mutations that prevent binding of phospholipase C-γ1 (LAT^{Y136F}) or Grb2 and Grap (LAT$^{Y175/195/236F}$) lead to lymphoproliferative disorders (16–18) dependent in the former case on RasGRP1-ERK signaling (19). These alleles collectively illustrate that both biochemical separation of function and quantitative loss of function mutations in a single pathway can lead to similar pathological outcomes (20).

A third critical node of proximal TCR signaling is controlled by the adapter protein SLP-76 (21), encoded in mice by the *Lcp2* gene. Null alleles of *Lcp2* prevent T cell development at an equivalent stage to LAT (22, 23), while a synthetic membrane-targeted version is associated with inflammatory cytokine production and autoantibodies (24). It is not clear if this association is the result of a biochemical separation or acquisition of function in SLP-76, or if it is due to a form of quantitative reduction in function similar to ZAP-70 (9).

Here we describe a splice variant of *Lcp2* that reduced the quantity of wild-type SLP-76 protein by approximately 90%. Homozygous mutants displayed a partial block in thymocyte development, with further impairments in negative selection and regulatory T cell development. Mutant mice developed spontaneous T_H1-biased effector T cells, accompanied by autoantibodies and elevated IgE and IgG1. The physiological outcomes of this mutation establish SLP-76 as a dose-sensitive node in the balance between immunity and immune dysregulation.

Materials & Methods

Mice

The *Lcp2*^{twimp} strain (MGI:3614800) was generated from a C57BL/6 male that received three weekly doses of 100 mg/kg *N*-ethyl-*N*-nitrosourea. Mutagenesis, mapping and sequencing methods have been described previously (25), as have 3A9 TCR transgenic (26), KLK4 *H-2K*^{b}:mHEL transgenic (27), NOD.*H2*^{k} (28), *Foxp3*$^{tm1.1Ayr}$ (29), *Foxp3*^{tm2Ayr} (*Foxp3*^{gfp}) (30), and C57BL/6.Ly5a congenic mice. *Lcp2*$^{twp/twp}$ *H2*^{k} mice were generated by breeding C57BL/6 *Lcp2*$^{twp/twp}$ (*H2*^{b}) mice with B10.BR (*H2*^{k}), and intercrossing F1 hybrids. Mice were housed in specific pathogen-free conditions at the Australian Phenomics Facility and Australian Cancer Research Facility (JCSMR), with all animal procedures approved by the Animal Ethics and Experimentation Committees of the Australian National University and University of Newcastle.

Flow cytometry

Lymphoid organ suspensions were prepared and stained with a combination of FITC-conjugated anti-CD4 (GK1.5), anti-CD44 (IM7), anti-CD69 (H1.2F3), anti-CD3ε (145-2C11), anti-TCRβ (H57-597); PE-conjugated anti-CD25 (7D4), anti-GITR (DTA-1) and anti-CD5 (53-7.3); PerCP-conjugated anti-CD8 (53-6.7); biotinylated anti-Vβ5 (MR9-4), anti-Vβ11 (RR3-15) and anti-TCRβ (H57-597); APC- or Qdot605-conjugated streptavidin; APC-conjugated anti-CD45.1 (A20) and anti-CCR7 (4B12); PE-Cy7 conjugated anti-CD24 (M1/69) and anti-CD8 (53-6.7) and Alexa700-conjugated anti-CD4 (GK1.5). Intracellular calcium after stimulation with anti-CD3ε (500A2) was measured using a mixture of Ly5-marked wild-type and mutant splenocytes labelled with Indo-1 (Molecular Probes). In some experiments, splenocytes were stimulated for 4h at 37°C in complete medium containing phorbol-12-myristate-13-acetate (PMA, 50ng/mL); ionomycin (1μM) and Golgistop (1:1500 v/v). Intracellular staining with anti-Foxp3-FITC (FJK-16s), anti-IFN-γ-FITC (XMG1.2), anti-IL-4-PE (11B11), anti-IL-17A-APC (eBio17B7) and anti-Helios-Pacific Blue (22F6) was performed using the Foxp3 Staining Buffer Set as per the manufacturer's instructions (eBioscience). 3A9 TCR bearing cells were identified by labelling cells with the clonotype-specific 1G12 hybridoma supernatant, followed by rat anti-mouse IgG1-APC (A85-1).

Western blotting

Whole thymocyte lysates prepared from *Lcp2*$^{+/+}$ and *Lcp2*$^{twp/twp}$ mice were subjected to SDS-PAGE, and Western blots probed with SLP-76 antiserum raised against an N-terminal peptide of SLP-76 (provided by G. Koretzky (31)). SLP-76 band intensity was measured by ImageJ.

Serology

Dilute serum (1:100) was incubated on HEp2 ANA slides (Inova), washed and incubated with FITC-conjugated anti-mouse IgG (Caltag). Slides were washed, mounted and fluorescence visualized and scored by a blinded individual. Measurement of serum immunoglobulins by ELISA was performed as previously described (9).

OVA challenge model

6- to 8-week-old mice were intraperitoneally injected with 50 μg ovalbumin (OVA) and 1 mg Rehydrogel (Reheis) in sterile saline. Mice were then challenged intranasally on days 12, 13, 14 and 15 with 10 μg OVA under isofluorane anesthesia. Mice were sacrificed 24 hours following the final challenge and serum collected by cardiac puncture. IgE was captured on plates coated with rat anti-mouse IgE (BD Biosciences), with total IgE detected by biotinylated rat anti-mouse IgE (BD Biosciences) and streptavidin-HRP (Biosource), and OVA-specific IgE detected with biotinylated OVA and streptavidin-HRP (Biosource).

Suppression assays

Performed as previously described (32). Briefly, CTV-labeled, FACS-purified $CD4^+CD44^{lo}CD62L^{hi}CD25^-$ splenocytes from CD45.1 mice ("responders") were co-cultured for 68 hours in round-bottomed 96-well plates with or without FACS-purified $CD3^-CD4^-CD8^-$ splenocytes from *Lcp2*$^{+/+}$ CD45.2 mice (APCs) and $CD4^+GFP^+$ splenocytes from *Lcp2*$^{+/+}$ or *Lcp2*$^{twp/twp}$ CD45.2 *Foxp3*^{gfp} mice (T-regs) in the presence of soluble anti-mouse CD3ε at 2ug/mL. At the start of the culture (day 0) each well contained 1.8×10^4 "responders" and the responder/APC ratio was either 1:5 or 1:2, held constant within a given experiment, and a range of responder/T-reg ratios were used, namely 1:1, 1:0.5 or 1:0.25 in each experiment.

Adoptive transfers

~3×10^7 unfractionated splenocytes were administered to 1 or 4 week-old recipient mice by intraperitoneal injection. Serum was collected 5–6 weeks post-transfer for the measurement of IgG autoantibodies, IgE and IgG1. For adoptive transfer of regulatory T cells, $CD45.1^+$*Foxp3*$^{-/-}$*Rag1*$^{-/-}$females were bred with CD45.1 C57BL/6 males to produce *Foxp3*$^{-/Y}$ mice, that were injected intraperitoneally at either 1 day or 7 days after birth with $1.25–2 \times 10^5$ FACS-sorted GFP^+ splenocytes from *Lcp2*$^{+/+}$ or *Lcp2*$^{twp/twp}$ CD45.2 *Foxp3*^{gfp} donor mice in 40uL PBS. Recipients were analysed at 19d or 28d after birth.

Results

T cell lymphopenia associated with a splice-donor mutation in Lcp2

In a genome-wide *N*-ethyl-*N*-nitrosourea screen for regulators of lymphocyte development (33), we identified several related individuals from a single pedigree with reduced frequencies of peripheral blood T cells and increased expression of the activation marker CD44 (Figure 1a,b,c). This phenotype, nicknamed '*twimp*' (*twp*), was inherited as a simple recessive Mendelian trait on a C57BL/6 background and when outcrossed to a NOD.*H2*^{k} mapping strain (Figure 1a).

To establish the chromosomal location of the *twimp* mutation we outcrossed *twimp* males (C57BL/6 background) to NOD.*H2*^{k} females and intercrossed the resulting F1 offspring (Figure 1a). From nine intercross breeder pairs, 152 offspring were screened for peripheral T cell deficiency and increased expression of CD44 by flow cytometry. Thirty-two individuals (21%) exhibited the *twimp* phenotype. Broad chromosomal linkage localised the mutation to an interval on chromosome 11, with fine mapping reducing the interval to between

D11Mit230 (27.90Mb) and D11Mit296 (43.63Mb) (Figure 1d). Within this interval lay *Lcp2*: the gene encoding SLP-76 (SH2 domain-containing leukocyte phosphoprotein of 76 kDa). *Lcp2* was a strong candidate for the *twimp* mutation, as SLP-76-deficient mice exhibit severe defects in T cell development (22, 23).

After sequencing all coding exons and flanking splice junctions of *Lcp2*, we identified a single intronic base substitution between C57BL/6 wild type and *twimp* mice (Figure 1e). The T to G transversion was located four bases downstream of the conserved 'GU/T' sequence, within the intronic splice donor site of intron 12. Amplification and sequencing of *Lcp2* cDNA from *twimp* splenocytes revealed the presence of both wild-type transcript and an aberrant transcript lacking exon 12 (Figure 1f). The absence of exon 12 is predicted to lead to a reading frame shift, introducing a premature termination codon within exon 13 (Figure 1f). This was reflected by a reduction of full-length SLP-76 protein expression in $Lcp2^{twp/twp}$ thymocytes (Figure 1g), with the Western blot band intensity estimated to be ~10% of wild-type. We detected no low molecular weight proteins using the same anti-SLP-76 antiserum raised against amino acids 136–235 (not depicted) (31), suggesting that the Δe12 splice product (or any other cryptic products) were not translated.

An early and partial arrest of thymic T cell development

$Lcp2^{twp/twp}$ thymi were consistently of lower cellularity than wild-type littermates, with significantly fewer DP ($CD4^+CD8^+$), CD4SP ($CD4^+CD8^-$) and CD8SP ($CD4^-CD8^+$) cells compared to $Lcp2^{+/+}$ controls (Figure 2a,b). Within the $CD4^-CD8^-$ (double negative, DN) thymocyte subset, $Lcp2^{twp/twp}$ mice had increased proportions and total numbers of DN3 ($CD44^-CD25^+$) cells, with fewer DN4 ($CD44^-CD25^-$) cells (Figure 2c,d), consistent with a defect in thymic β-selection. This partial block in T cell development was also apparent in the periphery, with $Lcp2^{twp/twp}$ mice showing reduced numbers of $CD4^+$, but not $CD8^+$, splenic T cells (Figure 2e,f).

During thymic positive selection the expression of CD5 increases, correlating positively with TCR signal intensity (34). Whereas CD5 expression was detectable on DP thymocytes from $Lcp2^{+/+}$ mice, CD5 expression on thymocytes from $Lcp2^{twp/twp}$ mice was significantly lower (Figure 2g). Positive selection of DP thymocytes also leads to an increase in expression of CD69, TCRβ and CD3ε. Compared to wild type controls, expression of CD69, TCRβ and CD3ε was significantly lower on $Lcp2^{twp/twp}$ DP thymocytes (Figure 2g). A partial block of $Lcp2^{twp/twp}$ thymocyte development and low expression of CD5, CD69, TCRβ and CD3ε on DP cells was consistent with a defect in TCR signaling and reduced SLP-76 function. Mixed bone marrow chimeras confirmed that the T lymphocyte deficiency was intrinsic to $Lcp2^{twp/twp}$ cells, as $Lcp2^{twp/twp}$ T cells were at a profound competitive disadvantage to wild-type (not depicted), and mutant peripheral T cells also exhibited severe functional impairments (Hillen et al., accompanying manuscript).

Immune dysregulation

In spite of the limited development of $Lcp2^{twp/twp}$ T cells and their impaired activation *in vitro*, unimmunized $Lcp2^{twp/twp}$ mice produced significantly more IgM, IgG1, IgG2b and IgE than their wild-type counterparts (Figure 3a), with IgG1 and IgE being especially high

(Figure 3b). In the case of IgE, this did not appear to be an exaggeration of antigen-specific responses, since sensitisation and challenge of *Lcp2*$^{twp/twp}$ mice with ovalbumin did not reveal any difference in ovalbumin-specific IgE secretion (Figure 3c). Elevated serum IgE and IgG1 was also accompanied by IgG autoantibodies against nuclear and cytoplasmic antigens, which were observed in 75% of *Lcp2*$^{twp/twp}$ mice, but only 6% of wild-type littermates (Figure 3d). Furthermore, intracellular staining after PMA+ionomycin stimulation revealed an increased frequency of IFN-γ-producing CD4$^+$ and CD8$^+$ splenocytes in *Lcp2*$^{twp/twp}$ mice. While the frequency of CD4$^+$ cells that produced IL-17A appeared elevated compared to wild-type, the difference was not statistically significant (Figure 3e).

Defective negative selection of Lcp2$^{twp/twp}$ T cells

TCRs with high affinity for self are normally purged from the thymocyte repertoire by negative selection, and defects at this stage can permit the escape of self-reactive clones that contribute to the onset of autoimmunity (35). To measure the efficiency of negative selection in *Lcp2*$^{twp/twp}$ mice, we used an *in vivo* model of superantigen-mediated deletion (36). Vβ5$^+$ and Vβ11$^+$ T cells that develop in the presence of the class II MHC molecule I-E^k (encoded by the *H2*^{k} haplotype) and certain endogenous mouse mammary tumor viruses are normally deleted in the thymus by negative selection. Yet in the absence of I-E^k (for example, in mice with the I-E^k-deficient *H2*^{b} haplotype) these same clonotypes are not deleted (Figure 4a). In *Lcp2*$^{twp/twp}$ mice, Vβ5$^+$ and Vβ11$^+$ T cells were inefficiently deleted in the presence of I-E^k (Figure 4a). CD4$^+$Vβ5$^+$ T cells can also be deleted in an I-E^k-independent manner (37), yet these cells were twice as prevalent in *H2*^{b} *Lcp2*$^{twp/twp}$ mice compared to *Lcp2*$^{+/+}$ controls (Figure 4a).

In addition to the relatively strong stimulus of superantigen-mediated deletion, we also measured deletion under a clonally-restricted setting using the hen egg lysozyme (HEL) peptide-specific 3A9 TCR transgene (class II-restricted). Positive selection was severely impaired in TCR transgenic *Lcp2*$^{twp/twp}$ mice, in which far fewer clonotype-positive (1G12$^+$) thymocytes and splenocytes were present (Figure 4b-c). To promote negative selection of these cells, the 3A9 TCR transgene was combined with a class I promoter-driven membrane-bound HEL antigen (abbreviated here as mHEL). In the presence of both transgenes (TCR$^+$mHEL$^+$), wild-type T cells are primarily deleted at the DP stage in the thymus, reducing DP numbers by ~99% and leaving very few clonotype-positive cells in the thymus or spleen (Figure 4b-c). Numbers of DP thymocytes were substantially higher in *Lcp2*$^{twp/twp}$ mice (Figure 4c), suggesting an impairment of negative selection. Upon closer examination however, the remaining DP, CD4SP and CD4$^+$ cells did not express the 1G12-reactive TCR transgene clonotype (Figure 4b-c), implying that negative selection was intact in this model.

A component of the thymocyte negative selection response that accompanies strong but not weak TCR signaling, and is separable from apoptosis, is upregulation of the Helios transcription factor (38). Using a CD24$^+$Foxp3$^-$ gate to exclude CD24$^-$ mature thymocytes and Foxp3$^+$ regulatory T cells, *Lcp2*$^{twp/twp}$ mice showed a 90% reduction in the frequency of TCRβ$^+$ thymocytes, consistent with the severe defect in αβ T cell positive selection

described above. However, the frequency of Helios$^+$ thymocytes within the small CD24$^+$Foxp3$^-$ TCRβ$^+$ population in *Lcp2$^{twp/twp}$* mice was increased relative to wild-type (Figure 4d-e). Consistent with a requirement for TCR-signaling in upregulation of Helios, *Zap70$^{mrd/mrt}$* mice analysed in parallel exhibited a decreased frequency of Helios$^+$ cells within their small CD24$^+$Foxp3$^-$TCRβ$^+$ thymocyte population (Figure 4d-e). These effects on Helios$^+$ cell frequencies were of similar magnitude in the immature CCR7$^-$ and semi-mature CCR7$^+$ subsets of TCRβ$^+$ thymocytes (data not shown). Thus, while these two mutations cripple both positive selection and clonal deletion in the thymus to similar degrees, a substantial fraction of nascent TCRβ$^+$ *Lcp2$^{twp/twp}$* thymocytes show evidence of registering a strong ZAP-70-dependent TCR signal as determined by Helios upregulation.

A second mode of thymus-acquired tolerance is the selection and activity of Foxp3$^+$ regulatory T cells (39). Numbers of CD4$^+$Foxp3$^+$ thymocytes were reduced in *Lcp2$^{twp/twp}$* mice (Figure 5a), yet splenic CD4$^+$Foxp3$^+$ cells were present in equivalent numbers and represented a greater proportion of total CD4$^+$ cells (Figure 5b). Expression of the IL-2 receptor alpha chain (CD25), but not the activation marker GITR, was also reduced on CD4$^+$Foxp3$^+$ splenocytes in *Lcp2$^{twp/twp}$* mice (Figure 5c). In order to test the suppressive function of *Lcp2$^{twp/twp}$* regulatory T cells, and to avoid complications of reduced CD25 expression, we sorted CD4$^+$GFP$^+$ cells from wild-type and mutant *Foxp3^{gfp}* reporter mice. After an initial experiment suggested a subtle suppression defect for *Lcp2$^{twp/twp}$* regulatory T cells, we repeated the experiment using fewer APCs. Under the latter conditions of reduced antigen presentation, a clear defect in suppression by *Lcp2$^{twp/twp}$* regulatory T cells was revealed (Figure 6a-b). Since IL-2 is critical for the survival of regulatory T cells (40), this reduction in CD25 expression, together with an imbalance between thymic output and peripheral numbers, may disrupt regulatory T cell function and contribute to dysregulated antibody production.

trans-acting reduction of IgE secretion in Lcp2$^{twp/twp}$ mice

Spontaneous production of IgE and IgG1 antibodies and IgG autoantibodies would commonly be suspected to arise from a dysregulation of helper T cell activity. In the case of *Lcp2$^{twp/twp}$* mice, impaired negative selection may allow the persistence and activation of autoreactive T cells, as would a disruption of Foxp3$^+$ regulatory T cell activity. T cell lymphopenia in *Lcp2$^{twp/twp}$* mice could also contribute to T cell hyperactivity through the excessive provision of survival factors such as IL-7, which oppose the upregulation of pro-apoptotic Bim by high-affinity TCR signals (41). During T cell lymphopenia IL-7 would be available in excess, increasing the amount of survival signal per cell and allowing the inappropriate survival and activation of self-reactive T lymphocytes.

To establish which of these *cis*- or *trans*-acting alternatives, if any, could explain immune dysregulation in *Lcp2$^{twp/twp}$* mice, we adoptively transferred wild-type splenocytes into young *Lcp2$^{twp/twp}$* recipients. Five weeks after transfer, serum IgE and IgG1 antibodies were both significantly reduced, indicating that a *trans*-acting mechanism was sufficient for the correction of immune dysregulation (Figure 7a).

Given their mode of action and reduced *in vitro* suppressive activity, we hypothesised that Foxp3$^+$ cells might account for the correction of antibody secretion after adoptive transfer.

Transfer of splenocytes from *Foxp3*-deficient mice did not lead to a reduction in IgE titres (Figure 7b), consistent with a need for Foxp3$^+$ regulatory T cells to suppress the excessive production of IgE in *Lcp2*$^{twp/twp}$ mice. However donor chimerism in the CD4$^+$ compartment was also less when *Foxp3*-deficient splenocytes were transferred, and was negatively correlated with serum IgE (Figure 7c), supporting the notion that CD4$^+$ cells were responsible for the *trans*-acting suppression of IgE. To directly test the consequences of adoptive transfer of Foxp3$^+$ cells, we sorted and injected cells from *Foxp3*^{gfp} reporter mice into *Foxp3*-deficient recipients. While wild-type Foxp3$^+$ cells engrafted successfully, those from *Lcp2*$^{twp/twp}$ donors did not (Figure 7d). This revealed that in addition to their impaired suppressive function, *Lcp2*$^{twp/twp}$ regulatory T cells were also poor engrafters.

Discussion

Each of us carries an abundance of rare and common variants in protein-coding genes, but we know little about which of these affect protein function. We know even less about the physiological consequences of such variants, which can often affect biological pathways in unpredictable ways. TCR signaling is one such pathway (20), and our analysis here reveals that a purely quantitative reduction of SLP-76 protein can disrupt immunity and tolerance to different degrees, resulting in immune dysregulation.

The *Lcp2*^{twimp} phenotype is clearly distinct from an exon 1 deletion of *Lcp2* (22, 23) where thymic development does not progress beyond the DN3 stage. It also differs from mice with phenylalanine substitutions at key tyrosine residues (Y145 or Y112/128), where a predicted disruption of Itk (in the case of Y145F) or Vav1 regulation (in the case of Y112/128F) leads to less severe positive selection defects and no indication of immune dysregulation (42, 43). This would suggest that a simple uncoupling of Vav1 or Itk pathways cannot explain the *Lcp2*^{twimp} phenotype, and that other qualitative or quantitative mechanisms may be responsible.

On the other hand, *Lcp2*$^{twp/twp}$ mice appear more similar to mice with a synthetic variant of SLP-76, in which the membrane-targeting sequence of LAT is fused to full-length SLP-76 (44). Like *Lcp2*$^{twp/twp}$, membrane-targeted SLP-76 mutants have moderate T cell lymphopenia and spontaneously produce autoantibodies, with peripheral T cells skewed towards the T_H1 and T_H17 lineages (24). These effects did not appear to be the result of skewed thymic selection, since adoptively transferred T cells from mice with a peripherally-induced mutation also produced more pro-inflammatory cytokines. Pro-inflammatory self-reactive T cells should also promote immune dysregulation in *cis*, so from our adoptive transfer experiments it would appear that defective negative selection was also not sufficient for excessive antibody production in *Lcp2*$^{twp/twp}$ mice. Nonetheless, the observation of defective superantigen-mediated deletion (and an increase in the frequency of Helios$^+$ thymocytes) implies that the *Lcp2*^{twimp} repertoire may be skewed towards higher self-reactivity, which could in turn be a necessary (but not sufficient) factor for immune dysregulation.

A mechanism that may be consistent between membrane-targeted SLP-76 mutants and *Lcp2*^{twimp} is the disrupted development and activity of Foxp3$^+$ regulatory T cells. In both

instances the proportion of $CD4^+$ cells that express Foxp3 was increased, yet expression of the IL-2 receptor alpha chain (CD25) was diminished. $CD4^+CD25^+$ cells from membrane-targeted mutants were as suppressive or less suppressive than wild-type cells *in vitro*, although the combined function of all $Foxp3^+$ cells ($CD25^{hi}$ and $CD25^{lo}$) was not determined as they were in our experiments (24). IL-2 and the IL-2R alpha chain (CD25) are both known to be essential for peripheral regulatory T cell homeostasis (40, 45, 46), making reduced CD25 expression a potential contributing factor to immune dysregulation in *Lcp2* mutants.

The *trans*-acting suppression of antibody production in $Lcp2^{twp/twp}$ mice was also consistent with an impairment of regulatory T cell function, with *Foxp3*-deficient splenocytes unable to suppress under the same conditions. How, then, might a quantitative reduction in SLP-76 protein disrupt regulatory T cell function? It is clear that thymic selection of $CD4^+Foxp3^+$ cells is dramatically reduced (perhaps due to an impairment of TCR signaling), yet their numbers are equivalent in the periphery. This extensive proliferative expansion from a limited pool of thymic emigrants may exhaust or restrict regulatory function, and might also account for the reduced expression of CD25 on peripheral $Lcp2^{twp/twp}$ $Foxp3^+$ cells. It is also consistent with other findings that homeostatic expansion of $Foxp3^+$ cells is independent of TCR signaling, as has been observed in mice with hypomorphic mutations in *Zap70* (9).

This proposed mechanism appears to be distinct from other variants in TCR signaling associated with immune dysregulation. $Zap70^{mrd/mrt}$ compound heterozygotes, for example, develop a similar combination of elevated IgE, IgG1 and autoantibodies (9). Yet reconstituting mice with a mixture of $Zap70^{mrd/mrt}$ and wild-type fetal liver cells did not reduce production of IgE (9). Less clear is the role of regulatory T cells in the pathology of LAT^{Y136F} mice: while transfer of $CD4^+CD25^+$ regulatory T cells into neonatal LAT^{Y136F} mice could prevent pathology (47), transfer of $CD4^+Foxp3^+$ cells could not (48). Furthermore, LAT^{Y136F} pathology does not seem to depend upon thymic selection processes nor an isolated loss of phospholipase C-γ1 binding, as peripheral deletion of LAT can also trigger lymphoproliferative disease (49). So despite falling within the same overarching pathway, variants of ZAP-70, LAT and SLP-76 appear to cause immune dysregulation by distinct mechanisms.

Immune dysregulation is not just a feature of mouse hypomorphic TCR signaling mutants, but is also a common characteristic of atypical human severe combined immunodeficiency (atypical SCID) (50). The genes mutated in atypical SCID are often the same as those in classical SCID (e.g. *RAG1*, *RAG2*, *ADA*, *IL2RG*, *LIG4* etc.), although the mutations are typically hypomorphic rather than null. Partial T lymphopenia, elevated IgE, and autoantibodies are all observed in atypical but not classical SCID (50), consistent with their mouse counterparts (20). Given the mechanistic distinctions between three hypomorphic mutants (*Zap70*, *Lat* and *Lcp2*) within a common pathway (TCR signaling), it is tempting to speculate that the mechanisms of immune dysregulation in atypical SCID patients are more heterogenous still.

Predicting the physiological effects of missense variants such as these will be a critical challenge for the future of human genetics. An even greater challenge will be to predict the effects of combinations of variants, such as compound heterozygous missense mutations at a single locus, or composite heterozygosity or homozygosity for several loci in a common pathway (51). Allelic variation in TCR signal transduction is a key illustration of this challenge, where hypomorphic variants at different points in the pathway can have paradoxical outcomes (20). Studying the effect of null alleles in mice and humans has defined our understanding of physiological gene function, as it has for TCR signaling, and will continue to do so (2). The use of mouse conditional alleles (52) and hypomorphic variants such as *Lcp2*^{twimp} (53, 54) will complement these efforts, and play an important role in understanding the immunological consequences of genetic variation between wild-type and null.

Acknowledgments

Supported by grants from the Wellcome Trust (082030/B/07/Z to CCG and 100083/Z/12/Z to OMS) the National Institutes of Health (R01 AI52127 and U54 AI054523 to CCG) and by a Program Grant and Australia Fellowship from the National Health and Medical Research Council (to CCG).

We thank Gary Koretzky for his gift of anti-SLP-76 polyclonal antibody, J. Fontenot and A. Rudensky for providing *Foxp3*$^{tm1.1Ayr}$ and *Foxp3*^{tm2Ayr} mice, and the staff of the Australian Phenomics Facility for genotyping and animal husbandry.

Abbreviations used in this paper

SLP-76	SH2 domain-containing leukocyte protein of 76 kilodaltons
Lcp2	lymphocyte cytosolic protein 2
ZAP-70	zeta-associated protein of 70 kilodaltons
SH2	Src-homology 2
LAT	linker for activated T cells

References

1. Siggs OM. Dissecting mammalian immunity through mutation. Immunol Cell Biol. 2014; 92:392–399. [PubMed: 24518983]
2. White JK, Gerdin A-K, Karp NA, Ryder E, Buljan M, Bussell JN, Salisbury J, Clare S, Ingham NJ, Podrini C, Houghton R, Estabel J, Bottomley JR, Melvin DG, Sunter D, Adams NC, Tannahill D, Logan DW, MacArthur DG, Flint J, Mahajan VB, Tsang SH, Smyth I, Watt FM, Skarnes WC, Dougan G, Adams DJ, Ramirez-Solis R, Bradley A, Steel KP. Genome-wide Generation and Systematic Phenotyping of Knockout Mice Reveals New Roles for Many Genes. Cell. 2013; 154:452–464. [PubMed: 23870131]
3. Samelson LE. Signal transduction mediated by the T cell antigen receptor: the role of adapter proteins. Annu Rev Immunol. 2002; 20:371–394. [PubMed: 11861607]
4. Negishi I, Motoyama N, Nakayama K, Nakayama K, Senju S, Hatakeyama S, Zhang Q, Chan AC, Loh DY. Essential role for ZAP-70 in both positive and negative selection of thymocytes. Nature. 1995; 376:435–438. [PubMed: 7630421]
5. Arpaia E, Shahar M, Dadi H, Cohen A, Roifman CM. Defective T cell receptor signaling and CD8+ thymic selection in humans lacking zap-70 kinase. Cell. 1994; 76:947–958. [PubMed: 8124727]

6. Elder ME, Lin D, Clever J, Chan AC, Hope TJ, Weiss A, Parslow TG. Human severe combined immunodeficiency due to a defect in ZAP-70, a T cell tyrosine kinase. Science. 1994; 264:1596–1599. [PubMed: 8202712]
7. Chan AC, Kadlecek TA, Elder ME, Filipovich AH, Kuo WL, Iwashima M, Parslow TG, Weiss A. ZAP-70 deficiency in an autosomal recessive form of severe combined immunodeficiency. Science. 1994; 264:1599–1601. [PubMed: 8202713]
8. Sakaguchi N, Takahashi T, Hata H, Nomura T, Tagami T, Yamazaki S, Sakihama T, Matsutani T, Negishi I, Nakatsuru S, Sakaguchi S. Altered thymic T-cell selection due to a mutation of the ZAP-70 gene causes autoimmune arthritis in mice. Nature. 2003; 426:454–460. [PubMed: 14647385]
9. Siggs OM, Miosge LA, Yates AL, Kucharska EM, Sheahan D, Brdicka T, Weiss A, Liston A, Goodnow CC. Opposing functions of the T cell receptor kinase ZAP-70 in immunity and tolerance differentially titrate in response to nucleotide substitutions. Immunity. 2007; 27:912–926. [PubMed: 18093540]
10. Yoshitomi H, Sakaguchi N, Kobayashi K, Brown GD, Tagami T, Sakihama T, Hirota K, Tanaka S, Nomura T, Miki I, Gordon S, Akira S, Nakamura T, Sakaguchi S. A role for fungal {beta}-glucans and their receptor Dectin-1 in the induction of autoimmune arthritis in genetically susceptible mice. J Exp Med. 2005; 201:949–960. [PubMed: 15781585]
11. Tanaka S, Maeda S, Hashimoto M, Fujimori C, Ito Y, Teradaira S, Hirota K, Yoshitomi H, Katakai T, Shimizu A, Nomura T, Sakaguchi N, Sakaguchi S. Graded attenuation of TCR signaling elicits distinct autoimmune diseases by altering thymic T cell selection and regulatory T cell function. J Immunol. 2010; 185:2295–2305. [PubMed: 20644168]
12. Peterson LK, Shaw LA, Joetham A, Sakaguchi S, Gelfand EW, Dragone LL. SLAP deficiency enhances number and function of regulatory T cells preventing chronic autoimmune arthritis in SKG mice. J Immunol. 2011; 186:2273–2281. [PubMed: 21248251]
13. Siggs OM, Yates AL, Schlenner S, Liston A, Lesage S, Goodnow CC. A ZAP-70 kinase domain variant prevents thymocyte-positive selection despite signalling CD69 induction. Immunology. 2014; 141:587–595. [PubMed: 24266404]
14. Cauwe B, Tian L, Franckaert D, Pierson W, Staats KA, Schlenner SM, Liston A. A novel Zap70 mutation with reduced protein stability demonstrates the rate-limiting threshold for Zap70 in T-cell receptor signalling. Immunology. 2014; 141:377–387. [PubMed: 24164480]
15. Zhang W, Sommers CL, Burshtyn DN, Stebbins CC, DeJarnette JB, Trible RP, Grinberg A, Tsay HC, Jacobs HM, Kessler CM, Long EO, Love PE, Samelson LE. Essential role of LAT in T cell development. Immunity. 1999; 10:323–332. [PubMed: 10204488]
16. Sommers CL, Park C-S, Lee J, Feng C, Fuller CL, Grinberg A, Hildebrand JA, Lacaná E, Menon RK, Shores EW, Samelson LE, Love PE. A LAT mutation that inhibits T cell development yet induces lymphoproliferation. Science. 2002; 296:2040–2043. [PubMed: 12065840]
17. Aguado E, Richelme S, Nuñez-Cruz S, Miazek A, Mura A-M, Richelme M, Guo X-J, Sainty D, He H-T, Malissen B, Malissen M. Induction of T helper type 2 immunity by a point mutation in the LAT adaptor. Science. 2002; 296:2036–2040. [PubMed: 12065839]
18. Nuñez-Cruz S, Aguado E, Richelme S, Chetaille B, Mura A-M, Richelme M, Pouyet L, Jouvin-Marche E, Xerri L, Malissen B, Malissen M. LAT regulates gammadelta T cell homeostasis and differentiation. Nat Immunol. 2003; 4:999–1008. [PubMed: 12970761]
19. Kortum RL, Rouquette-Jazdanian AK, Miyaji M, Merrill RK, Markegard E, Pinski JM, Wesselink A, Nath NN, Alexander CP, Li W, Kedei N, Roose JP, Blumberg PM, Samelson LE, Sommers CL. A phospholipase C-γ1-independent, RasGRP1-ERK-dependent pathway drives lymphoproliferative disease in linker for activation of T cells-Y136F mutant mice. J Immunol. 2013; 190:147–158. [PubMed: 23209318]
20. Liston A, Enders A, Siggs OM. Unravelling the association of partial T-cell immunodeficiency and immune dysregulation. Nat Rev Immunol. 2008; 8:545–558. [PubMed: 18551129]
21. Jordan MS, Koretzky GA. Coordination of receptor signaling in multiple hematopoietic cell lineages by the adaptor protein SLP-76. Cold Spring Harb Perspect Biol. 2010; 2:a002501. [PubMed: 20452948]

22. Pivniouk V, Tsitsikov E, Swinton P, Rathbun G, Alt FW, Geha RS. Impaired viability and profound block in thymocyte development in mice lacking the adaptor protein SLP-76. Cell. 1998; 94:229–238. [PubMed: 9695951]
23. Clements JL, Yang B, Ross-Barta SE, Eliason SL, Hrstka RF, Williamson RA, Koretzky GA. Requirement for the leukocyte-specific adapter protein SLP-76 for normal T cell development. Science. 1998; 281:416–419. [PubMed: 9665885]
24. Sonnenberg GF, Mangan PR, Bezman NA, Sekiguchi DR, Luning Prak ET, Erikson J, Maltzman JS, Jordan MS, Koretzky GA. Mislocalization of SLP-76 leads to aberrant inflammatory cytokine and autoantibody production. Blood. 2010; 115:2186–2195. [PubMed: 20029045]
25. Miosge LA, Blasioli J, Blery M, Goodnow CC. Analysis of an ethylnitrosourea-generated mouse mutation defines a cell intrinsic role of nuclear factor kappaB2 in regulating circulating B cell numbers. J Exp Med. 2002; 196:1113–1119. [PubMed: 12391023]
26. Ho WY, Cooke MP, Goodnow CC, Davis MM. Resting and anergic B cells are defective in CD28-dependent costimulation of naive CD4+ T cells. J Exp Med. 1994; 179:1539–1549. [PubMed: 7909325]
27. Hartley SB, Crosbie J, Brink R, Kantor AB, Basten A, Goodnow CC. Elimination from peripheral lymphoid tissues of self-reactive B lymphocytes recognizing membrane-bound antigens. Nature. 1991; 353:765–769. [PubMed: 1944535]
28. Lesage S, Hartley SB, Akkaraju S, Wilson J, Townsend M, Goodnow CC. Failure to censor forbidden clones of CD4 T cells in autoimmune diabetes. J Exp Med. 2002; 196:1175–1188. [PubMed: 12417628]
29. Fontenot JD, Gavin MA, Rudensky AY. Foxp3 programs the development and function of CD4+CD25+ regulatory T cells. Nat Immunol. 2003; 4:330–336. [PubMed: 12612578]
30. Fontenot JD, Fontenot JD, Rasmussen JP, Rasmussen JP, Williams LM, Williams LM, Dooley JL, Dooley JL, Farr AG, Farr AG, Rudensky AY, Rudensky AY. Regulatory T cell lineage specification by the forkhead transcription factor foxp3. Immunity. 2005; 22:329–341. [PubMed: 15780990]
31. Clements JL, Ross-Barta SE, Tygrett LT, Waldschmidt TJ, Koretzky GA. SLP-76 expression is restricted to hemopoietic cells of monocyte, granulocyte, and T lymphocyte lineage and is regulated during T cell maturation and activation. J Immunol. 1998; 161:3880–3889. [PubMed: 9780153]
32. Altin JA, Goodnow CC, Cook MC. IL-10+CTLA-4+ Th2 Inhibitory Cells Form in a Foxp3-Independent, IL-2-Dependent Manner from Th2 Effectors during Chronic Inflammation. J Immunol. 2012; 188:5478–5488. [PubMed: 22547705]
33. Nelms KA, Goodnow CC. Genome-wide ENU mutagenesis to reveal immune regulators. Immunity. 2001; 15:409–418. [PubMed: 11567631]
34. Azzam HS, Grinberg A, Lui K, Shen H, Shores EW, Love PE. CD5 expression is developmentally regulated by T cell receptor (TCR) signals and TCR avidity. J Exp Med. 1998; 188:2301–2311. [PubMed: 9858516]
35. Siggs OM, Makaroff LE, Liston A. The why and how of thymocyte negative selection. Curr Opin Immunol. 2006; 18:175–183. [PubMed: 16459069]
36. Kappler JW, Roehm N, Marrack P. T cell tolerance by clonal elimination in the thymus. Cell. 1987; 49:273–280. [PubMed: 3494522]
37. Fink PJ, Fang CA, Turk GL. The induction of peripheral tolerance by the chronic activation and deletion of CD4+V beta 5+ cells. J Immunol. 1994; 152:4270–4281. [PubMed: 7908916]
38. Daley SR, Hu DY, Goodnow CC. Helios marks strongly autoreactive CD4+ T cells in two major waves of thymic deletion distinguished by induction of PD-1 or NF-κB. J Exp Med. 2013; 210:269–285. [PubMed: 23337809]
39. Hori S, Nomura T, Sakaguchi S. Control of regulatory T cell development by the transcription factor Foxp3. Science. 2003; 299:1057–1061. [PubMed: 12522256]
40. Liston A, Siggs OM, Goodnow CC. Tracing the action of IL-2 in tolerance to islet-specific antigen. Immunol Cell Biol. 2007; 85:338–342. [PubMed: 17372610]
41. Strasser A, Bouillet P. The control of apoptosis in lymphocyte selection. Immunol Rev. 2003; 193:82–92. [PubMed: 12752673]

42. Jordan MS, Smith JE, Burns JC, Austin J-ET, Nichols KE, Aschenbrenner AC, Koretzky GA. Complementation in trans of altered thymocyte development in mice expressing mutant forms of the adaptor molecule SLP76. Immunity. 2008; 28:359–369. [PubMed: 18342008]
43. Smith-Garvin JE, Burns JC, Gohil M, Zou T, Kim JS, Maltzman JS, Wherry EJ, Koretzky GA, Jordan MS. T-cell receptor signals direct the composition and function of the memory CD8+ T-cell pool. Blood. 2010; 116:5548–5559. [PubMed: 20847203]
44. Bezman NA, Baker RG, Lenox LE, Jordan MS, Koretzky GA. Cutting edge: rescue of pre-TCR but not mature TCR signaling in mice expressing membrane-targeted SLP-76. J Immunol. 2009; 182:5183–5187. [PubMed: 19380761]
45. Fontenot JD, Rasmussen JP, Gavin MA, Rudensky AY. A function for interleukin 2 in Foxp3-expressing regulatory T cells. Nat Immunol. 2005; 6:1142–1151. [PubMed: 16227984]
46. D'Cruz LM, Klein L. Development and function of agonist-induced CD25+Foxp3+ regulatory T cells in the absence of interleukin 2 signaling. Nat Immunol. 2005; 6:1152–1159. [PubMed: 16227983]
47. Koonpaew S, Shen S, Flowers L, Zhang W. LAT-mediated signaling in CD4+CD25+ regulatory T cell development. J Exp Med. 2006; 203:119–129. [PubMed: 16380508]
48. Wang Y, Kissenpfennig A, Mingueneau M, Richelme S, Perrin P, Chevrier S, Genton C, Lucas B, DiSanto JP, Acha-Orbea H, Malissen B, Malissen M. Th2 lymphoproliferative disorder of LatY136F mutant mice unfolds independently of TCR-MHC engagement and is insensitive to the action of Foxp3+ regulatory T cells. J Immunol. 2008; 180:1565–1575. [PubMed: 18209052]
49. Mingueneau M, Roncagalli R, Grégoire C, Kissenpfennig A, Miazek A, Archambaud C, Wang Y, Perrin P, Bertosio E, Sansoni A, Richelme S, Locksley RM, Aguado E, Malissen M, Malissen B. Loss of the LAT adaptor converts antigen-responsive T cells into pathogenic effectors that function independently of the T cell receptor. Immunity. 2009; 31:197–208. [PubMed: 19682930]
50. Felgentreff K, Perez-Becker R, Speckmann C, Schwarz K, Kalwak K, Markelj G, Avcin T, Qasim W, Davies EG, Niehues T, Ehl S. Clinical and immunological manifestations of patients with atypical severe combined immunodeficiency. Clin Immunol. 2011; 141:73–82. [PubMed: 21664875]
51. Andrews TD, Sjollema G, Goodnow CC. Understanding the immunological impact of the human mutation explosion. Trends Immunol. 2013; 34:99–106. [PubMed: 23333204]
52. Skarnes WC, Rosen B, West AP, Koutsourakis M, Bushell W, Iyer V, Mujica AO, Thomas M, Harrow J, Cox T, Jackson D, Severin J, Biggs P, Fu J, Nefedov M, de Jong PJ, Stewart AF, Bradley A. A conditional knockout resource for the genome-wide study of mouse gene function. Nature. 2011; 474:337–342. [PubMed: 21677750]
53. Andrews TD, Whittle B, Field MA, Balakishnan B, Zhang Y, Shao Y, Cho V, Kirk M, Singh M, Xia Y, Hager J, Winslade S, Sjollema G, Beutler B, Enders A, Goodnow CC. Massively parallel sequencing of the mouse exome to accurately identify rare, induced mutations: an immediate source for thousands of new mouse models. Open Biol. 2012; 2:120061. [PubMed: 22724066]
54. Arnold CN, Barnes MJ, Berger M, Blasius AL, Brandl K, Croker B, Crozat K, Du X, Eidenschenk C, Georgel P, Hoebe K, Huang H, Jiang Z, Krebs P, La Vine D, Li X, Lyon S, Moresco EMY, Murray AR, Popkin DL, Rutschmann S, Siggs OM, Smart NG, Sun L, Tabeta K, Webster V, Tomisato W, Won S, Xia Y, Xiao N, Beutler B. Sanger Institute Mouse Genetics Project. ENU-induced phenovariance in mice: inferences from 587 mutations. BMC Res Notes. 2012; 5:577. [PubMed: 23095377]

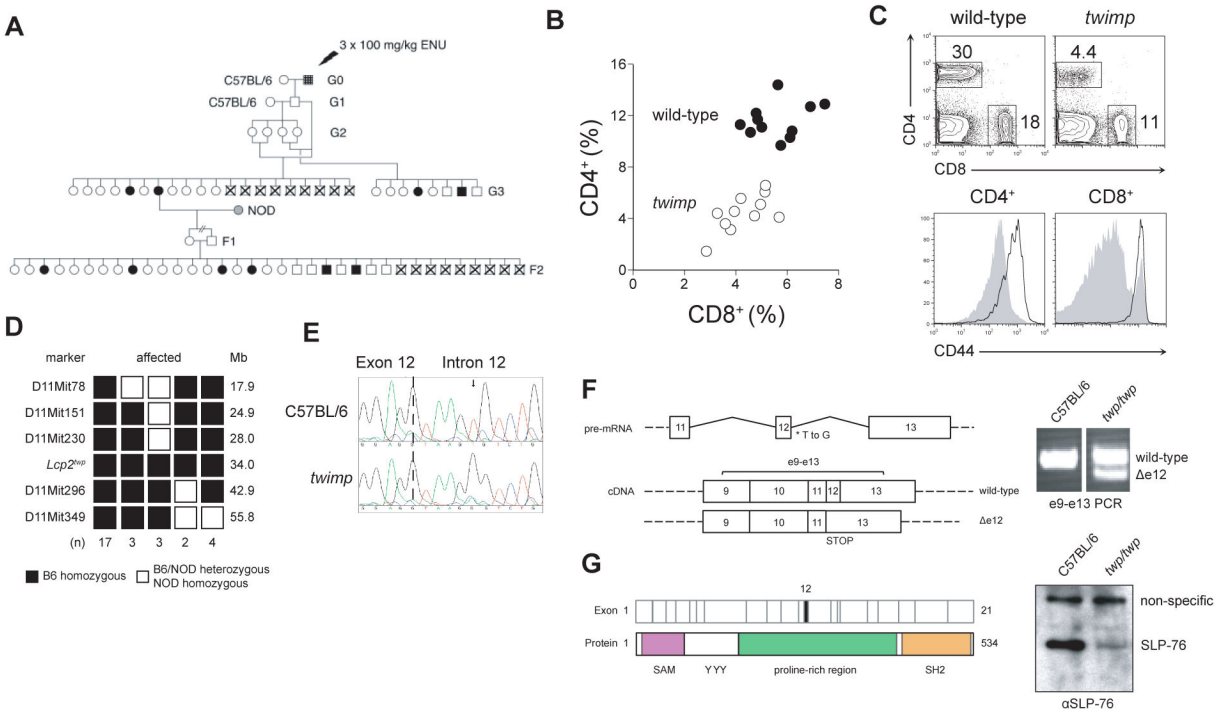

Figure 1. Identification and mapping of the *twimp* mutation

A) Initial generations of the *twimp* pedigree showing individuals that were affected (filled), unaffected (open) or not typed (cross) for the T cell phenotype. B) Definition of the *twimp* phenotype by $CD4^+$ and $CD8^+$ cell frequency in blood. C) Representative flow cytometry profiles measuring frequencies of $CD4^+$ and $CD8^+$ cells, and histogram overlays comparing expression of CD44 on $CD4^+$ and $CD8^+$ cells in lymph nodes. D) Fine mapping of the *twimp* mutation on chromosome 11. Haplotypes of individual *twimp* affected mice are shown in columns – C57BL/6 homozygote (black squares); C57BL/6-NOD.$H2^k$ heterozygote or NOD.$H2^k$ homozygote (white squares). Numbers of individual mice with each haplotype are indicated at the base of each column. E) Amplified genomic DNA from *twimp* mice was used to sequence *Lcp2*, revealing a T to G transversion within intron 12. F) Representative location of the *twimp* mutation in *Lcp2*, and its effect on *Lcp2* RNA processing: sequencing of *twimp* cDNA revealed the presence of two transcripts: one full-length and a second that lacked exon 12. Right hand panel shows the products of a PCR reaction (forward primer in exon 9, reverse in exon 13) performed on splenic cDNA from C57BL/6J and *twimp* mice. G) Schematic representation of the SLP-76 protein and the coding contribution of each exon, with the exon deleted in *twimp* (e12) shown in black. Expression of SLP-76 protein was measured by probing thymocyte lysates from with a polyclonal anti-SLP-76 antibody. SAM, sterile alpha motif; YYY, tyrosines 112/128/145; SH2, Src homology 2.

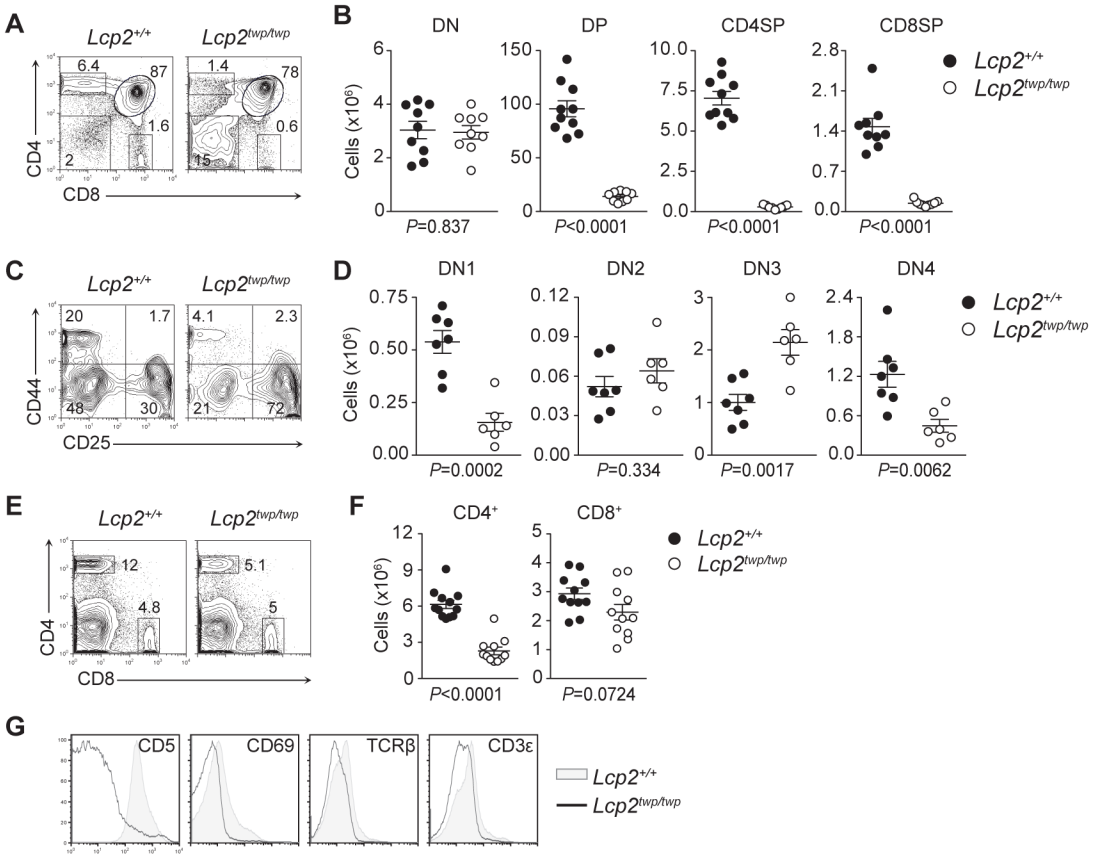

Figure 2. Impaired development and function of *Lcp2*$^{twp/twp}$ T cells

A) Representative flow cytometry plots of CD4 and CD8 expression on thymocytes from *Lcp2*$^{+/+}$ and *Lcp2*$^{twp/twp}$ mice, showing frequencies of each subset. B) Absolute numbers of DN (CD4^{-}CD8^{-}), DP (CD4^{+}CD8^{+}), CD4SP (CD4^{+}CD8^{-}) and CD8SP (CD4^{-}CD8^{+}) thymocytes. C) Representative flow cytometry plots of CD25 and CD44 expression on DN (CD4^{-}CD8^{-}) thymocytes from *Lcp2*$^{+/+}$ and *Lcp2*$^{twp/twp}$ mice, resolving DN1 (CD44^{+}CD25^{-}), DN2 (CD44^{+}CD25^{+}), DN3 (CD44^{-}CD25^{+}) and DN4 cells (CD44^{-}CD25^{-}). D) Absolute numbers of DN1-DN4 thymocytes. Representative flow cytometry plots showing percentages (E) and absolute numbers (F) of CD4^{+} and CD8^{+} splenic lymphocytes. G) Representative histogram overlays of CD69, CD5, TCRβ and CD3ε expression on DP thymocytes from *Lcp2*$^{+/+}$ (filled, grey) and *Lcp2*$^{twp/twp}$ (open, red) histograms. Data are representative of (A,C,E,G) or pooled from (B,D,F) two independent experiments. Symbols represent individual mice, while bars represent mean and standard error. *P* values were calculated by 2-tailed unpaired Student's t-test.

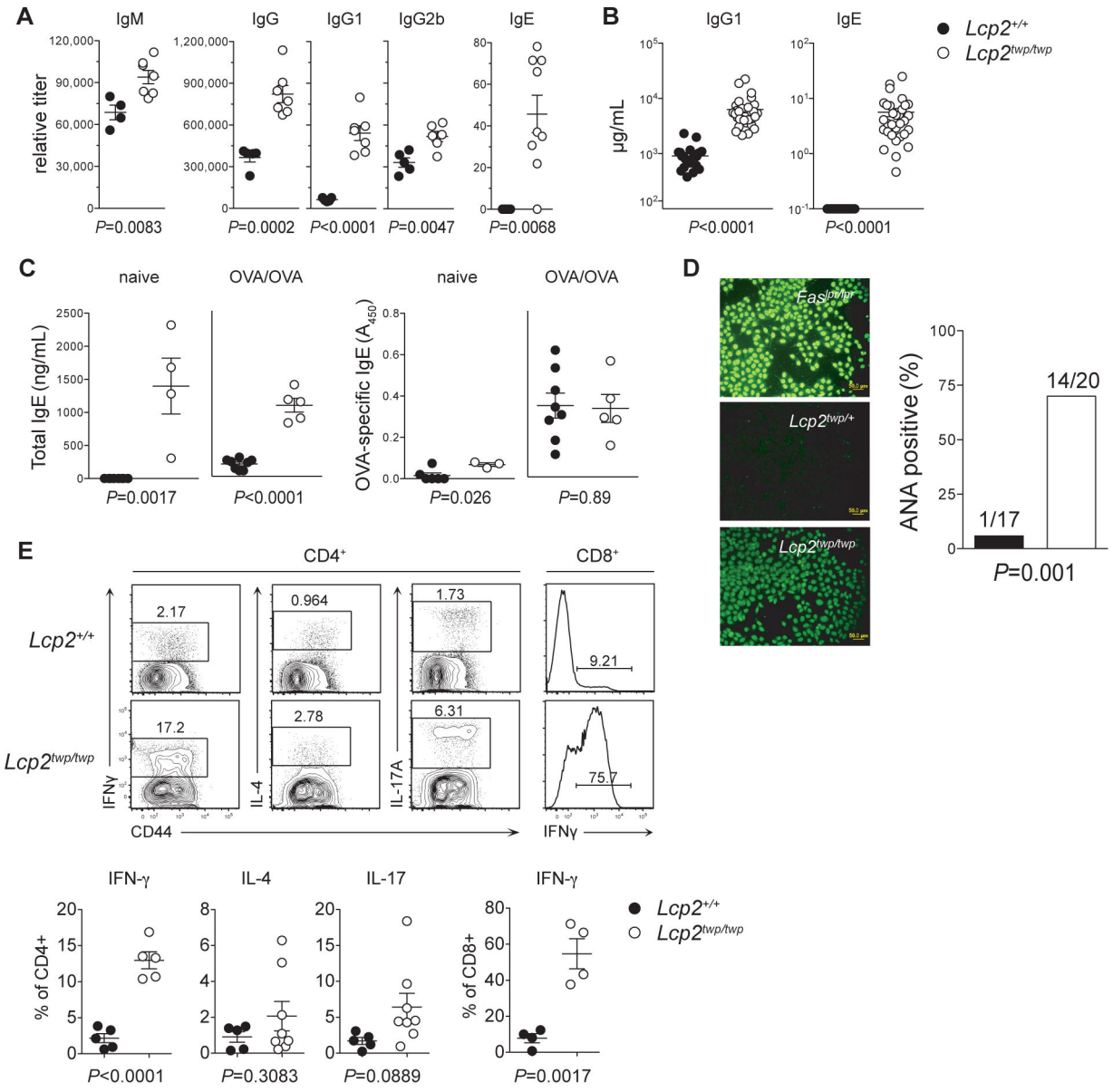

Figure 3. Spontaneous immune dysregulation in *Lcp2*$^{twp/twp}$ mice

A) Relative titers of serum immunoglobulins as measured by ELISA. B) Replicated IgG1 and IgE concentration measurements. C) Relative titres of total (left) and OVA-specific IgE (right). OVA/OVA groups were sensitised i.p., then challenged intranasally with ovalbumin. D) Representative HEp2 slides incubated with sera from 8–15 week-old *Fas*$^{lpr/lpr}$ (positive control), *Lcp2*$^{+/twp}$ or *Lcp2*$^{twp/twp}$ mice, followed by incubation with anti-mouse IgG-FITC. Bar graph indicates the proportion of 8–15 week-old autoantibody-positive *Lcp2*$^{+/twp}$ or *Lcp2*$^{twp/twp}$ mice. E) Representative flow cytometry plots (top) and frequencies (bottom) of IFN-γ, IL-4 or IL-17 expression in CD4$^+$ and CD8$^+$ splenocytes 4h after stimulation with PMA and ionomycin. Symbols represent individual mice, while bars represent mean and standard error. *P* values were calculated by Mann-Whitney test (A & B [IgE], C [total IgE naive], D) or 2-tailed unpaired Student's t-test (A, B, C, E).

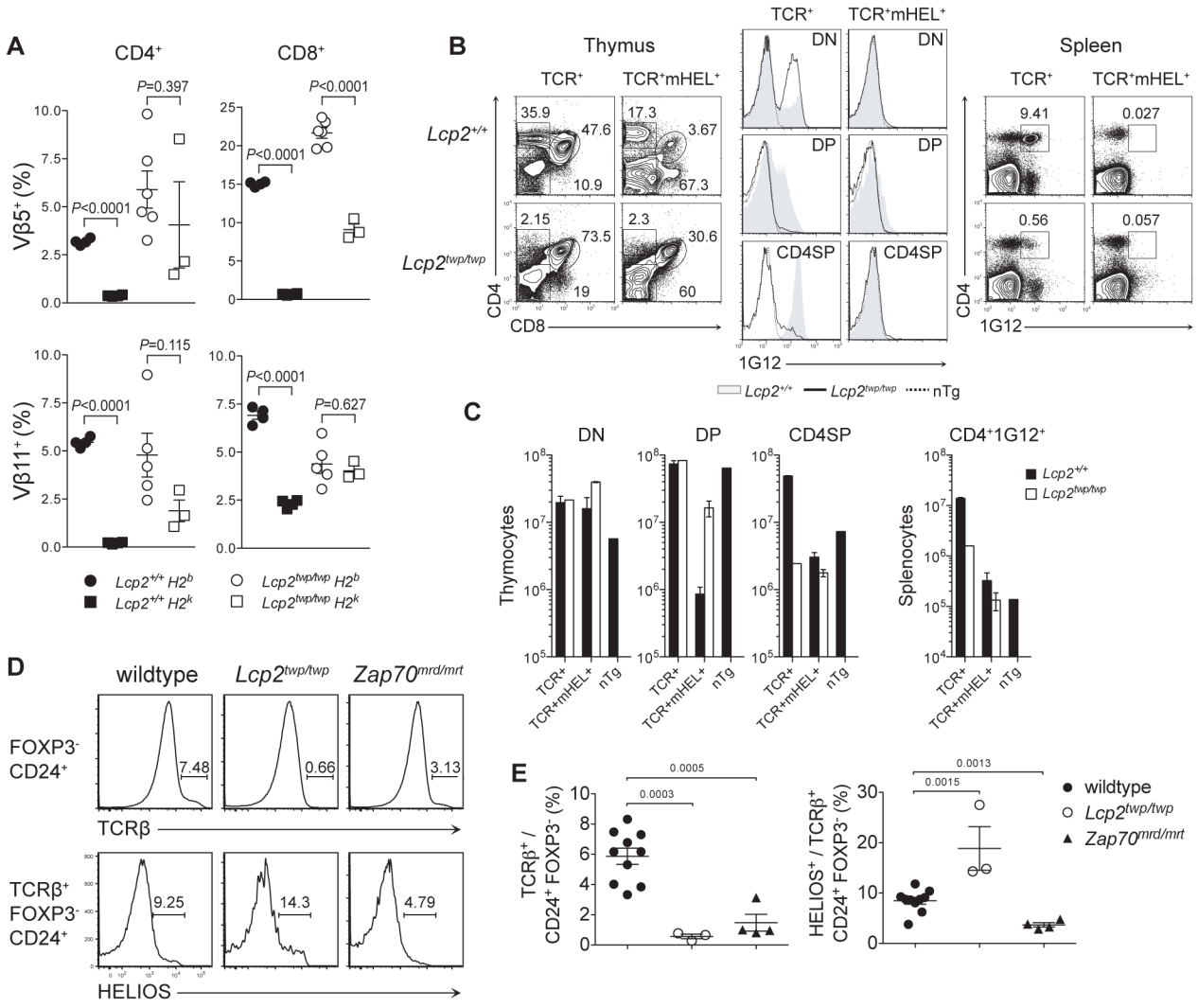

Figure 4. Negative selection in *Lcp2*$^{twp/twp}$ mice

A) Percentages of CD4$^+$ and CD8$^+$ peripheral blood lymphocytes that were Vβ11$^+$ or Vβ5$^+$ were compared between *H2*^{b} and *H2*^{k} genetic backgrounds. B) Thymocytes and splenocytes from 3A9 TCR transgenic (TCR$^+$) or 3A9 TCR;mHEL double transgenic (TCR$^+$mHEL$^+$) mice were analysed by flow cytometry, and absolute numbers of DN (CD4$^-$CD8$^-$), DP (CD4$^+$CD8$^+$), CD4SP (CD4$^+$CD8$^-$) and CD4$^+$1G12$^+$) were calculated (C). D) Flow cytometry of CD24$^+$Foxp3$^-$ thymocytes from wild-type, *Lcp2*$^{twp/twp}$ or *Zap70*$^{mrd/mrt}$ mice showing a gate for the TCRβ$^+$ subset (top), amongst which the frequency of Helios$^+$ cells was enumerated (bottom). E) Frequencies of the indicated populations were calculated from the histograms presented in (D). Symbols represent individual mice, while bars represent mean and standard error. *P* values were calculated by 2-tailed unpaired Student's t-test.

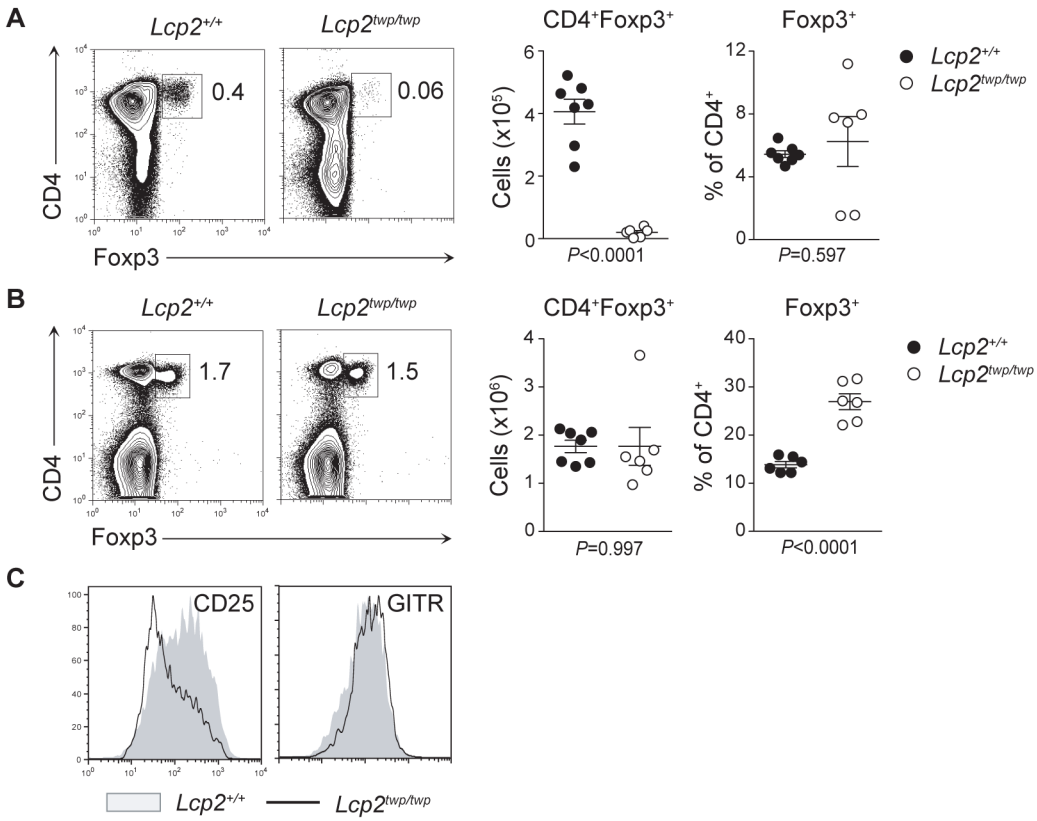

Figure 5. Development of Foxp3$^+$ cells in *Lcp2$^{twp/twp}$* mice

Representative flow cytometry plots and absolute numbers of CD4$^+$Foxp3$^+$ thymocytes (A) or splenocytes (B). C) Representative histogram overlays of CD25 and GITR expression upon CD4$^+$Foxp3$^+$ splenic lymphocytes from *Lcp2$^{+/+}$* (filled) and *Lcp2$^{twp/twp}$* (open) mice. Symbols represent individual mice, while bars represent mean and standard error. *P* values were calculated by 2-tailed unpaired Student's t-test.

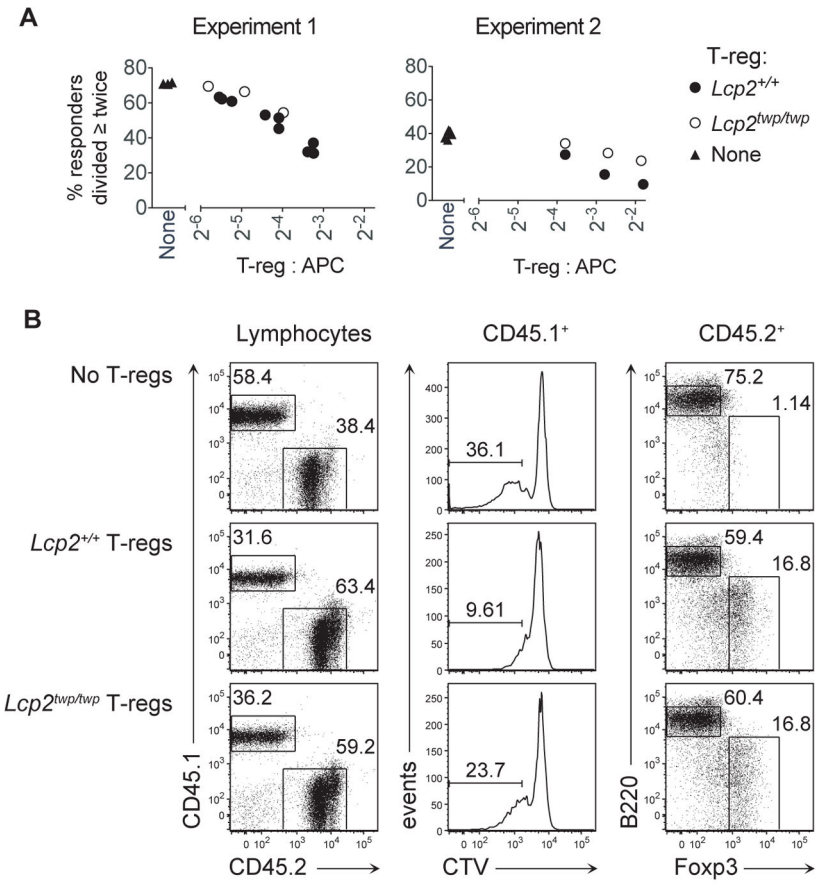

Figure 6. Impaired function of *Lcp2*$^{twp/twp}$ Foxp3^{+} cells

A) Proliferation of FACS-purified CD4^{+}CD44^{lo}CD62L^{hi}CD25^{-} responders (CD45.1), after 68 hours of stimulation with soluble anti-CD3. Responders were cultured in the presence of FACS-purified CD3^{-}CD4^{-}CD8^{-} cells (APCs, C57BL/6, CD45.2) and CD4^{+}GFP^{+} cells (T-regs, CD45.2) from *Lcp2*$^{+/+}$ or *Lcp2*$^{twp/twp}$ *Foxp3*^{gfp} mice. (B) Flow cytometry plots from experiment 2 (T-reg:APC ratio of 2^{-2}).

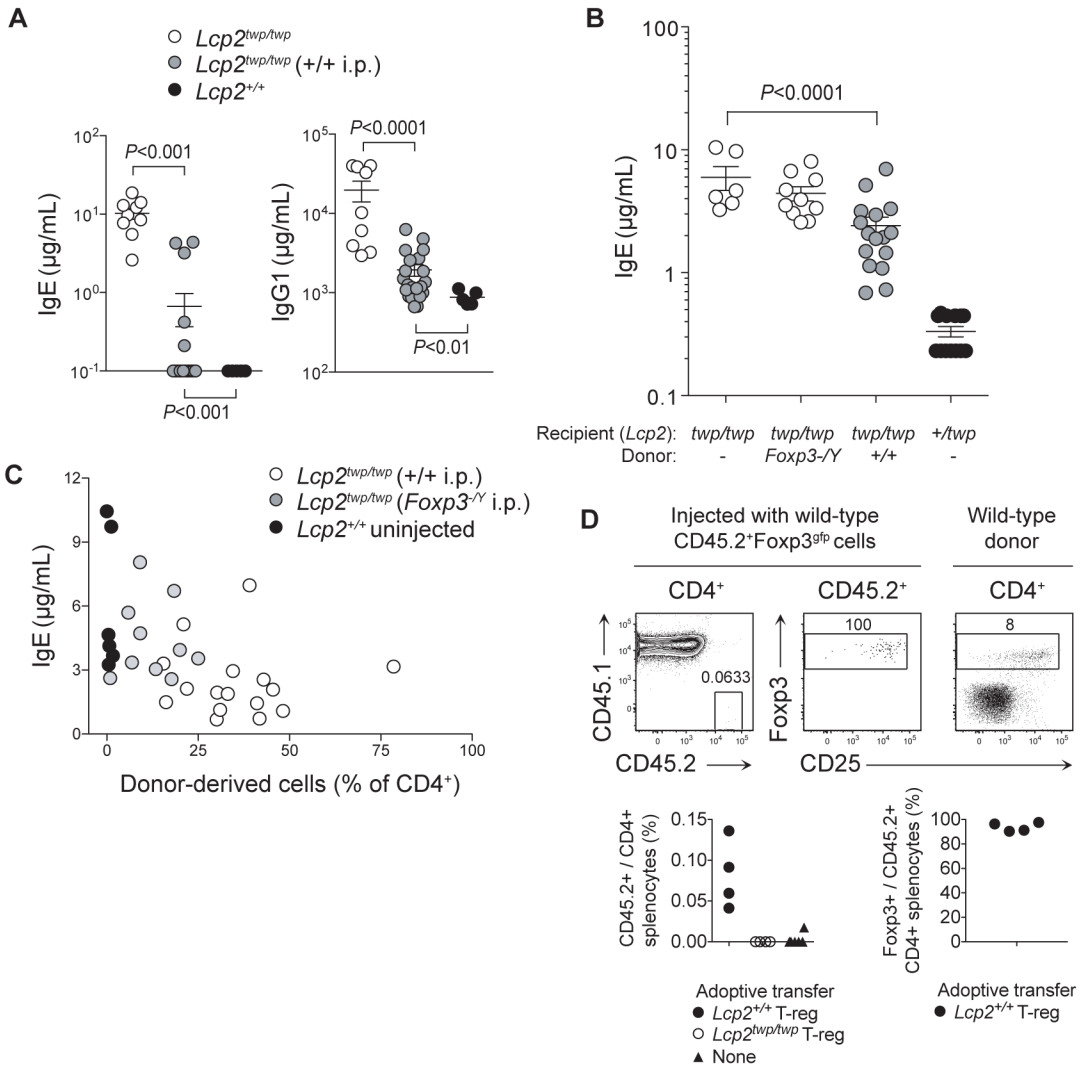

Figure 7. Correction of *Lcp2*$^{twp/twp}$ serological phenotypes by adoptive transfer of *Lcp2*$^{+/+}$ splenocytes

A) 1–4 week-old *Lcp2*$^{twp/twp}$ mice received intraperitoneal injections of ~3×10^7 whole splenocytes from *Lcp2*$^{+/+}$ donors (*Lcp2*$^{twp/twp}$ (+/+ i.p.)), or did not receive any donor splenocytes (*Lcp2*$^{twp/twp}$, *Lcp2*$^{+/+}$). Recipients were sacrificed 5 weeks post-transfer and serum was assayed for the presence of IgE and IgG1 antibodies. (B,C) CD45.2$^+$ *Lcp2*$^{twp/twp}$ mice aged 6–11 weeks were left unmanipulated or were injected i.v. with ~2×10^7 splenocytes from CD45.1$^+$ *Foxp3*$^{+/y}$ or *Foxp3*$^{-/y}$ littermate mice aged 2–3 weeks. Peripheral blood was collected 3–6 weeks after adoptive transfer and serum IgE concentration was measured by ELISA (shown in B) and is plotted as a function of the frequency of CD45.1$^+$ donor cells amongst CD4$^+$ cells (in C). D) *Foxp3*$^{-/Y}$ mice (CD45.1) were injected intraperitoneally at 1 or 7 days of age with 1.25–2 × 10^5 FACS-sorted GFP$^+$ splenocytes from *Lcp2*$^{+/+}$ or *Lcp2*$^{twp/twp}$ *Foxp3*^{gfp} donors (CD45.2), with donor CD4$^+$ engraftment measured at 19 or 28 days of age. Results are pooled from two independent experiments. Symbols represent individual mice, while bars represent mean and standard error. *P* values

were calculated by a Kruskal-Wallis test followed by Dunn's multiple comparison test (A [IgE]), or one-way ANOVA followed by Bonferroni's multiple comparison test (A [IgG1]).